NUMERICAL SIMULATION OF DEEP-WELL WET OXIDATION REACTOR USING STEAM

By S. Mittal,[1] H. A. Deans,[2] and T. E. Tezduyar[3]

ABSTRACT: A finite element model is developed for the numerical simulation of the start-up of a deep-well wet oxidation reactor using steam. The model is capable of handling different cases of start-up, using saturated steam of arbitrary quality including hot water. The transient temperature field in the well-earth system is studied. The governing equation for the earth is the conductive heat equation. For the reactor, the analysis involves solving the energy balance equations describing the convective and intertube heat transfer, mass balance equations, and thermodynamic relations for the fluid in the tubes. The equations for the reactor and the earth are coupled by the continuity of the temperature and heat flux at the interface between them. A Galerkin finite element formulation is used for the spatial discretization of the heat equation in the earth; a Petrov-Galerkin finite element formulation is employed for the energy balance equations in the reactor tubes. The resulting set of ordinary differential equations is discretized in time and solved by a predictor-multicorrector algorithm. The model is tested on a typical deep-well reactor to study its start-up dynamics. The results can be used to estimate the start-up time and the amount of steam or water required to obtain the necessary initiation temperature for the process.

INTRODUCTION

A finite element simulation of a deep-well wet oxidation process for treating dilute aqueous waste streams was earlier reported by Liou et al. (1990). We now extend the model to simulate the start-up of the reactor by injecting saturated steam of arbitrary quality, or hot water, through the "steam tube." The saturated steam goes through a phase change due to heat exchange with the neighboring tube. This necessitates the inclusion of certain other thermodynamic relations to be solved for the steam tube, which we describe later in this paper.

A possible configuration of the deep-well reactor is shown in Fig. 1. The well consists of an outer casing that contains the reactor assembly of concentric tubes. The central tube carries steam to the lower section of the reactor for start-up heating. The second concentric tube delivers the oxygen down to the lower section of the reactor once the reaction is initiated. The slurry of water and waste enters the well by the third (down) tube, turns the corner at the bottom, and exits by the fourth (up) tube. During the start-up, only water is fed through the down tube.

Before initiating the oxidation reaction, the reactor must be preheated to the desired starting temperature. The present design uses high-pressure steam injected down hole to achieve this objective. The high-pressure steam is injected at a given quality $\epsilon_0^s(t)$ and temperature $T_0^s(t)$. It condenses due to

[1]Res. Asst., Dept. of Aerosp. Engrg. and Mech., and Minnesota Supercomputer Inst., Univ. of Minnesota, Minneapolis, MN 55455.

[2]Prof., Dept. of Chem. and Petroleum Engrg., Univ. of Wyoming, Laramie, WY 82071.

[3]Assoc. Prof., Dept. of Aerosp. Engrg. and Mech., and Minnesota Supercomputer Inst., University of Minnesota, Minneapolis, MN 55455.

Note. Discussion open until September 1, 1991. To extend the closing date one month, a written request must be filed with the ASCE Manager of Journals. The manuscript for this paper was submitted for review and possible publication on July 14, 1990. This paper is part of the ***Journal of Engineering Mechanics***, Vol. 117, No. 4, April, 1991. ©ASCE, ISSN 0733-9399/91/0004-0798/$1.00 + $.15 per page. Paper No. 25702.

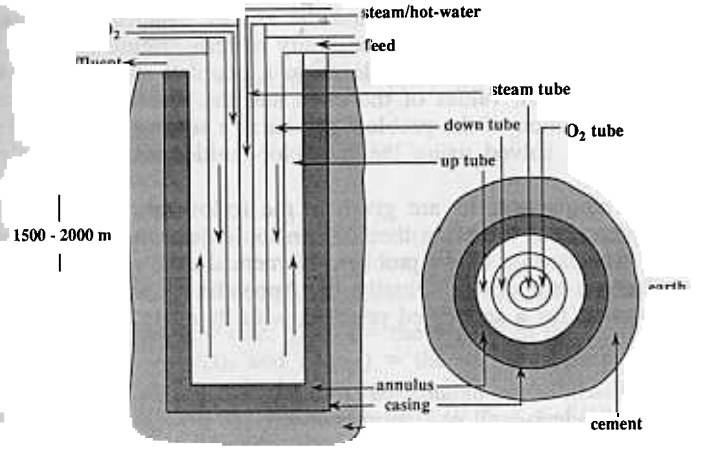

FIG. 1. Deep-Well Sludge Oxidation Reactor Configuration

the heat exchange with the inner tube, and mixes with the down-flowing stream at the bottom of the reactor. During the start-up procedure, no oxygen is injected; thus, no fluid flows in the corresponding tube. As a result, the heat transfer coefficient between the steam pipe and the down pipe is relatively small. In some cases, the steam does not condense entirely before reaching the bottom of the reactor. In other cases total condensation occurs. We also study the case in which hot water is injected to preheat the reactor.

It is assumed that temperature variation in the cross section of the tubes is negligible compared with the gradients along the length of the well. Therefore we model the reactor one-dimensionally. In the steam tube, pressure is assumed to be caused only by the hydrostatic head, i.e., friction is neglected. In the case in which high-pressure saturated steam is injected, the temperature of the fluid in the steam tube is found to be a function of the pressure from steam tables. This temperature is then used to find the thermodynamic properties for the vapor and the liquid phases. This information is used in conjunction with the heat and the mass balance equations to calculate the quality of the mixture, iteratively. Once the quality and other thermodynamic properties of the saturated mixture are known, we use the finite element formulation to solve for the temperature. In the case in which the steam tube fluid is not in the saturated state, the thermodynamic properties are functions of both temperature and pressure in the steam tube. We use the hydrostatic pressure and the predicted value of temperature from the previous time step to evaluate the thermodynamic properties. Certain physical properties of the fluid in the down and up tubes are assumed to be constant.

The heat transfer in the reactor tubes is convection-dominated. It is well known that in such cases the Galerkin formulation leads to spurious node-to-node oscillations. The Petrov-Galerkin finite element method provides a robust numerical performance compared with the Galerkin method in convection-dominated problems (Brooks and Hughes 1982; Tezduyar and Ganjoo 1986). Therefore, we employ a Petrov-Galerkin finite element formulation for the spatial discretization of the energy balance equations for the reactor tubes. We use the regular Galerkin finite element formulation for the spatial discretization of the conductive heat equation for the earth.

The heat equation in the earth and the energy balance equations in the reactor tubes are coupled by the continuity of temperature and heat flux at the interface between them. This leads to a coupled system involving the unknown temperature values of the earth and the reactor tubes. The finite element discretization of the problem results in a set of ordinary differential equations that is solved using the predictor-multicorrector time algorithm (Hughes 1987).

The governing equations are given in the following, in which a proper scaling is performed to obtain their dimensionless forms. Next, we discuss the spatial discretization of the problem. Numerical examples are then solved, and conclusions are drawn. Finally, in Appendix I, we compare the numerical solution for a simplified problem with its analytical solution.

Problem Statement

We now consider the balance equations and the thermodynamic relations involved in the deep-well oxidation process (see Fig. 2 for a schematic reactor profile). These equations consist of energy-balance equations for the fluid in all the reactor tubes, a conductive heat equation for the surrounding earth strata, a mass balance equation, a pressure equation, and thermodynamic relations for the steam tube.

For the earth, the heat equation in cylindrical coordinates, assuming no angular variation, is

$$(\rho C_p)_E \frac{\partial T_E}{\partial t} = \kappa \left[\frac{1}{r} \frac{\partial}{\partial r} \left(r \frac{\partial T_E}{\partial r} \right) + \frac{\partial^2 T_E}{\partial z^2} \right] \quad \ldots\ldots (1)$$

where $T_E(r,z,t)$ = the temperature of the earth; and κ and $(\rho C_p)_E$ = the thermal conductivity and volumetric heat capacity of the earth, respectively.

The equations describing the heat balance in the reactor tubes are

for the down tube:

$$(A\rho C_p)_F + (A\rho C_p)_F \frac{\partial T_F}{\partial t} + (\dot{m} C_p)_F^d \frac{\partial T_F}{\partial x} \cdot (\sigma U)^{sd}(T_F^d - T_F^s)$$

$$\sigma U)^{ud}(T_F^d - T_F^u) = S, \qquad 0 \le x \le H$$

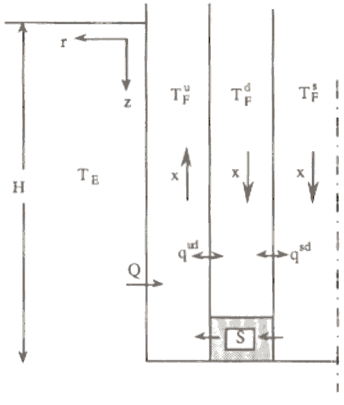

FIG. 2. Schematic of Simplified Reactor Profile

for the up tube:

$$[(A\rho C_p)_F^u + (A\rho C_p)_P^u]\frac{\partial T_F^u}{\partial t} + (\dot{m}C_p)_F^u\frac{\partial T_F^u}{\partial x} + (\sigma U)^{ud}(T_F^u - T_F^d) = Q,$$

$$H \le x \le 2H \quad \ldots\ldots (3)$$

for the steam tube:

$$[(A\rho C_p)_P^s]\frac{\partial T_F^s}{\partial t} + A_F^s\frac{\partial}{\partial t}(\rho_F^s\hat{h}_F^s) + \frac{\partial}{\partial x}(\dot{m}_F^s\hat{h}_F^s) + (\sigma U)^{sd}(T_F^s - T_F^d) = 0,$$

$$0 \le x \le H \quad \ldots\ldots (4)$$

where $\dot{m}$ = the mass flow rate; $\rho_F^s(x,t)$ = the density of the fluid in the steam tube; and $T_F^d(x,t)$, $T_F^s(x,t)$, and $T_F^u(x,t)$ = the temperatures of the fluids in the down, steam, and up tubes, respectively. Here x = the linear coordinate along the tubes in the direction of the flow ($0 \le x \le 2H$), and H = the depth of the well. It starts from the inlet of the down and steam tubes, goes to the bottom of the reactor, turns the corner, and ends at the exit of the up tube. The heat capacity per unit length of the fluid in tube and the tube itself (i.e., the pipe) is denoted by $(A\rho C_p)_F$ and $(A\rho C_p)_P$, respectively. The flow rate of heat capacity is denoted by $(\dot{m}C_p)_F$; this term can also be expressed as $(A\rho C_p)_F\bar{V}$, where $\bar{V}$ = the average velocity of the fluid; and A = the cross-sectional area. The heat transfer area (per unit length of the tube) and the overall heat transfer coefficient between the tubes are represented by σ and U, respectively. The superscripts *sd* and *ud* refer to the interaction between the steam and down tubes and the up and down tubes, respectively. The specific enthalpy of the steam tube fluid is denoted by h_F^s. The heat flux from the earth to the reactor, and the heat added by the steam during start-up, both defined per unit length of the tube, are denoted by $Q(x,t)$, and $S(x,t)$.

Mass balance for the fluid in the steam tube is given as

$$A_F^s\frac{\partial\rho_F^s}{\partial t} + \frac{\partial\dot{m}_F^s}{\partial x} = 0, \qquad 0 \le x \le H \quad \ldots\ldots (5)$$

Mass flow rate in the up tube is determined by the mass balance of the fluids at the bottom of the reactor

$$\dot{m}_F^u(t) = \dot{m}_F^d + \dot{m}_F^s(H,t) \quad \ldots\ldots (6)$$

where $\dot{m}_F^d$ = the mass flow rate of the fluid in the down tube, assumed to be constant; and $\dot{m}_F^u(t)$ = the flow rate in the up tube.

In the steam tube, the hydrostatic pressure $p_F^s(x,t)$, neglecting friction, is given by

$$\frac{\partial p_F^s}{\partial x} = \rho_F^s g, \qquad 0 \le x \le H \quad \ldots\ldots (7)$$

where g = the acceleration due to gravity.

To solve the problem completely, we also need certain thermodynamic relations for the fluid in the steam tube. For water (single phase), specific enthalpy and density are functions of temperature and pressure

$$\hat{h}_F^s = \hat{h}_F^s(T_F^s, p_F^s) \quad \ldots\ldots (8a)$$

$$\rho_F^s = \rho_F^s(T_F^s, p_F^s) \quad \ldots\ldots (8b)$$

From Eqs. 4, 5, and 8*a*, the energy equation for the steam tube fluid in single phase is

$$\left[(A\rho C_p)_P^s + A_F^s\rho_F^s\left(\frac{\partial\hat{h}_F^s}{\partial T_F^s}\right)_{p_F^s}\right]\frac{\partial T_F^s}{\partial t} + \dot{m}_F^s\left(\frac{\partial\hat{h}_F^s}{\partial T_F^s}\right)_{p_F^s}\frac{\partial T_F^s}{\partial x} + (\sigma U)^{sd}(T_F^s - T_F^d)$$

$$= -\left(\frac{\partial\hat{h}_F^s}{\partial p_F^s}\right)_{T_F^s}\left[(A\rho)_F^s\frac{\partial p_F^s}{\partial t} + \dot{m}_F^s\frac{\partial p_F^s}{\partial x}\right], \qquad 0 \le x \le H \quad \ldots\ldots (9)$$

For the case in which the steam tube fluid is in the saturation state (two-phase system), the quality of the saturated steam $\epsilon_F^s(x,t)$ comes in as an independent variable. Quality is defined as the ratio of the mass of vapor to the total mass of liquid and vapor when the substance is in a saturation state. The temperature of the mixture in this case becomes a function of the saturation pressure

$$T_F^s = T_F^s(p_F^s) \quad \ldots\ldots (10)$$

The specific enthalpy of the saturated water vapor system can be expressed in terms of the quality ϵ_F^s, the specific enthalpy of the vapor $\hat{h}_v(T_F^s)$, and the specific enthalpy of the liquid $\hat{h}_l(T_F^s)$ in the mixture

$$\hat{h}_F^s = \hat{h}_v\epsilon_F^s + \hat{h}_l(1 - \epsilon_F^s) \quad \ldots\ldots (11)$$

$$\hat{h}_v = \hat{h}_v(T_F^s) \quad \ldots\ldots (12a)$$

$$\hat{h}_l = \hat{h}_l(T_F^s) \quad \ldots\ldots (12b)$$

Similarly, the density of the saturated water vapor system can be expressed in terms of the quality ϵ_F^s, the density of the vapor $\rho_v(T_F^s)$, and the density of the liquid $\rho_l(T_F^s)$ in the mixture

$$\rho_F^s = \rho_v\epsilon_F^s + \rho_l(1 - \epsilon_F^s) \quad \ldots\ldots (13)$$

$$\rho_v = \rho_v(T_F^s) \quad \ldots\ldots (14a)$$

$$\rho_l = \rho_l(T_F^s) \quad \ldots\ldots (14b)$$

Data for Eqs. 8*a*, 8*b*, 10, 12*a*, 12*b*, 14*a*, and 14*b* are available in the steam tables (McLintock and Silvestri 1968). From Eqs. 4, 5, and 11, the energy equation for the steam tube fluid in saturation state is

$$\left[(A\rho C_p)_P^s + A_F^s\rho_F^s\left(\frac{\partial\hat{h}_F^s}{\partial T_F^s}\right)_{\epsilon_F^s}\right]\frac{\partial T_F^s}{\partial t} + \dot{m}_F^s\left(\frac{\partial\hat{h}_F^s}{\partial T_F^s}\right)_{\epsilon_F^s}\frac{\partial T_F^s}{\partial x} + (\sigma U)^{sd}(T_F^s - T_F^d)$$

$$= -\left(\frac{\partial\hat{h}_F^s}{\partial\epsilon_F^s}\right)_{T_F^s}\left[(A\rho)_F^s\frac{\partial\epsilon_F^s}{\partial t} + \dot{m}_F^s\frac{\partial\epsilon_F^s}{\partial x}\right], \qquad 0 \le x \le H \quad \ldots\ldots (15)$$

where, from Eq. 11

$$\left(\frac{\partial\hat{h}_F^s}{\partial T_F^s}\right)_{\epsilon_F^s} = \epsilon_F^s\frac{d\hat{h}_v}{dT_F^s} + (1 - \epsilon_F^s)\frac{d\hat{h}_l}{dT_F^s} \quad \ldots\ldots (16a)$$

$$\left(\frac{\partial\hat{h}_F^s}{\partial\epsilon_F^s}\right)_{T_F^s} = \hat{h}_v - \hat{h}_l \quad \ldots\ldots (16b)$$

The boundary and initial conditions for the earth and the tubes are given as

$$T_E(r_0,z,t) = T_F^u(2H - z,t), \qquad \text{for } 0 \le z \le H, \qquad t \ge 0 \qquad (17)$$

$$T_E(h,z,t) = T_E^0(z), \qquad \text{for } 0 \le z \le H + h, \qquad t \ge 0 \ldots. \qquad (18)$$

$$T_E(r,H+h,t) = T_E^0(H+h), \quad \text{for } 0 \le r \le h, \quad t \ge 0 \ldots\ldots \quad (19)$$

$$\frac{\partial T_E}{\partial r}(0,z,t) = 0, \quad \text{for } H \le z \le H+h, \quad t \ge 0 \quad (20)$$

$$\frac{\partial T_E}{\partial z}(r,0,t) = 0, \quad \text{for } r_0 \le r \le h, \quad t \ge 0 \quad (21)$$

$$T_F^d(0,t) = T_E^0(0), \quad \text{for } t \ge 0 \ldots\ldots (22a)$$

$$T_F^s(0,t) = T_0^s(t), \quad \text{for } t \ge 0 \ldots\ldots (22b)$$

$$T_E(r,z,0) = T_E^0(z), \quad \text{for } 0 \le z \le H, \quad r_0 \le r \le h,$$
$$H \le z \le H+h, \quad 0 \le r \le h \ldots\ldots (23)$$

$$T_F^d(x,0) = T_E^0(x), \quad \text{for } 0 \le x \le H \ldots\ldots (24a)$$

$$T_F^s(x,0) = T_E^0(x), \quad \text{for } 0 \le x \le H \ldots\ldots (24b)$$

$$T_F^u(x,0) = T_E^0(2H-x), \quad \text{for } H \le x \le 2H \ldots\ldots (25)$$

$$\dot{m}_F^s(0,t) = \dot{m}_0^s(t), \quad \text{for } t \ge 0 \ldots\ldots (26a)$$

$$\dot{m}_F^d(t) = \dot{m}_0^d(t), \quad \text{for } t \ge 0 \ldots\ldots (26b)$$

An additional constraint on the temperature of the fluids at the bottom of the reactor is given as

$$T_F^u(H,t) - T_E^s(H,t) = T_F^d(H,t), \quad \text{for } t \ge 0 \ldots\ldots (27)$$

It should be noted that it is possible to avoid this constraint by writing an explicit energy balance at the bottom of the reactor to calculate the temperature in the up tube at that point.

For the inlet conditions for the steam tube, we also specify, for single phase (i.e., when water is injected)

$$p_F^s(0,t) = p_0^s(t), \quad \text{for } t \ge 0 \ldots\ldots (28)$$

and for two phase (i.e., when saturated steam is injected)

$$\epsilon_F^s(0,t) = \epsilon_0^s(t), \quad \text{for } t \ge 0 \ldots\ldots (29)$$

Here r_0 = the radius of the outer casing of the reactor, h = the heat penetration distance beyond which heat effect is negligible; $T_E^0(z)$ = the natural temperature profile in the earth; and $T_0^s(t)$, $\dot{m}_0^s(t)$, $p_0^s(t)$, and $\epsilon_0^s(t)$ = the temperature, mass flow rate, pressure, and quality of the fluid at the inlet of the steam tube, respectively. The heat flux Q at the interface of the earth and the up tube is

$$Q = 2\pi\kappa\left(r\frac{\partial T_E}{\partial r}\right)\Big|_{r=r_0} \ldots\ldots (30)$$

Dividing Eq. 1 by $(\rho C_p)_E$ and Eqs. 2, 3, 9, and 15 by $(A\rho C_p)_F^d$, and by using the scaling

$$\theta = \frac{T - T_E^0(0)}{T_{max} - T_E^0(0)} = \frac{T - T_E^0(0)}{(\Delta T)_{max}} \quad (31)$$

$$r^* = \frac{r}{h} \quad (32a)$$

$$x^* = \frac{x}{H} \quad (32b)$$

$$z^* = \frac{z}{H}, \qquad \text{for } 0 \le z \le H \tag{33a}$$

$$z^* = 1 + \frac{z - H}{h}, \qquad \text{for } H \le z \le H + h \tag{33b}$$

$$t^* = \frac{t}{\left(\frac{h^2}{\alpha}\right)} \tag{34a}$$

$$\alpha = \frac{\kappa}{(\rho C_p)_E} \tag{34b}$$

we obtain the following dimensionless forms

$$\frac{\partial \theta_E}{\partial t^*} = \frac{1}{r^*}\frac{\partial}{\partial r^*}\left(r^* \frac{\partial \theta_E}{\partial r^*}\right) + \frac{1}{L^2}\frac{\partial^2 \theta_E}{\partial z^{*2}} \tag{35}$$

$$(f_p)^d \frac{\partial \theta_F^d}{\partial t^*} + \frac{(\mathrm{Pe})^d}{L}\frac{\partial \theta_F^d}{\partial x^*} + (\beta^*)^{ud}(\theta_F^d - \theta_F^u) + (\beta^*)^{sd}(\theta_F^d - \theta_F^s) = \Sigma^*,$$

$$\text{for } 0 \le x^* \le 1 \tag{36}$$

$$(f_p)^u \frac{\partial \theta_F^u}{\partial t^*} + \frac{(\mathrm{Pe})^u}{L}\frac{\partial \theta_F^u}{\partial x^*} + (\beta^*)^{ud}(\theta_F^u - \theta_F^d) = 2\pi\gamma^*\left(r^* \frac{\partial \theta_E}{\partial r^*}\right)\Big|_{r^* = r_0^*},$$

$$\text{for } 1 \le x^* \le 2 \tag{37}$$

$$(f_p)^s \frac{\partial \theta_F^s}{\partial t^*} + \frac{(\mathrm{Pe})^s}{L}\frac{\partial \theta_F^s}{\partial x^*} + (\beta^*)^{sd}(\theta_F^s - \theta_F^d) = (P^*)^s, \qquad \text{for } 0 \le x^* \le \tag{38}$$

wnere

$$(f_p)^d = \frac{(A\rho C_p)_P^d}{(A\rho C_p)_F^d} + 1 \ldots\ldots \tag{39a}$$

$$(f_p)^u = \frac{(A\rho C_p)_P^u + (A\rho C_p)_F^u}{(A\rho C_p)_F^d} \tag{39b}$$

$$(f_p)^s = \frac{(A\rho C_p)_P^s + A_F^s \rho_F^s \left(\dfrac{\partial h_F^s}{\partial T_F^s}\right)_{P_F^s}}{(A\rho C_p)_F^d} \qquad \text{for single phase} \tag{40}$$

$$(f_p)^s = \frac{(A\rho C_p)_P^s + A_F^s \rho_F^s \left(\dfrac{\partial \hat{h}_F^s}{\partial T_F^s}\right)_{e_F^s}}{(A\rho C_p)_F^d}, \qquad \text{for two phase} \tag{41}$$

$$(\mathrm{Pe})^d = \frac{h\dot{m}_F^d}{\alpha(A\rho)_F^d} \ldots \tag{42a}$$

$$(\mathrm{Pe})^u = \frac{h(\dot{m}C_p)_F^u}{\alpha(A\rho C_p)_F^d} \tag{42b}$$

$$(\mathrm{Pe})^s = \frac{h\dot{m}_F^s \left(\frac{\partial \hat{h}_F^s}{\partial T_F^s}\right)_{p_F^s}}{\alpha(A\rho C_p)_F^d}, \qquad \text{for single phase} \qquad \ldots (43)$$

$$(\mathrm{Pe})^s = \frac{h\dot{m}_F^s \left(\frac{\partial \hat{h}_F^s}{\partial T_F^s}\right)_{\epsilon_F^s}}{\alpha(A\rho C_p)_F^d}, \qquad \text{for two phase} \qquad (44)$$

$$(\beta^*)^{ud} = \frac{h^2(\sigma U)^{ud}}{\alpha(A\rho C_p)_F^d}$$

$$(\beta^*)^{sd} = \frac{h^2(\sigma U)^{sd}}{\alpha(A\rho C_p)_F^d}$$

$$\Sigma^* = \frac{h^2 S}{\alpha(\Delta T)_{\max}(A\rho C_p)_F^d} \qquad (46a)$$

$$S = \frac{[\dot{m}_F^s \epsilon_F^s (h_u - \hat{h}_l)](H - D, t)}{D}$$

$$\gamma^* = \frac{h^2 \kappa}{\alpha(A\rho C_p)_F^d} \qquad \ldots\ldots (47)$$

$$(P^*)^s = \frac{-h^2 \left(\frac{\partial \hat{h}_F^s}{\partial p_F^s}\right)_{T_F^s} \left[(A\rho)_F^s \frac{\partial p_F^s}{\partial t} + \dot{m}_F^s \frac{\partial p_F^s}{\partial x}\right]}{\alpha(\Delta T)_{\max}(A\rho C_p)_F^d} \qquad \text{for single phase} \qquad (48)$$

$$(P^*)^s = \frac{-h^2 \left(\frac{\partial \hat{h}_F^s}{\partial \epsilon_F^s}\right)_{T_F^s} \left[(A\rho)_F^s \frac{\partial \epsilon_F^s}{\partial t} + \dot{m}_F^s \frac{\partial \epsilon_F^s}{\partial x}\right]}{\alpha(\Delta T)_{\max}(A\rho C_p)_F^d} \qquad \text{for two phase} \qquad (49)$$

$$L = 1, \qquad \text{for } 1 < z^*$$

$$L = \frac{H}{h}, \qquad \text{for } 0 < z^* < 1, \qquad 0 \le x^* \le 2 \ldots . \qquad \ldots . (50)$$

In Eq. 46*b*, D = the distance over which the heat is added. In the numerical example we consider we take D as one element length. This value can later be modified once we know more about the mixing at the bottom of the reactor. Note that two different length scales are used, and that $H/h >> 1$. The well depth H is used for the linear coordinate x along the tubes and the coordinate z above depth H in the earth. The heat penetration distance h is used to scale the radial coordinate and the coordinate z below the depth H in the earth

Spatial Discretization

Let Ω_E denote the computational domain for the earth and $\mathbf{E}_E$ denote the set of elements resulting from the discretization of Ω_E into subdomains Ω_E^e, $e = 1, 2, \ldots, \mathrm{nel}_E$ where nel_E = the number of elements in Ω_E. The following finite dimensional spaces associated with $\mathbf{E}_E$ are defined:

$$V^h(\Omega_E) = [w^h | w^h \in H^{1h}(\Omega_E), \qquad w^h = 0 \quad \text{on } \Gamma_g] \ldots\ldots\ldots\ldots\ldots\ldots (51)$$

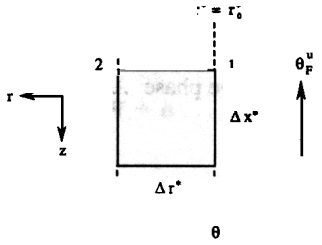

FIG. 3. Typical Earth Element Adjacent to Reactor

$$S^h(\Omega_E) = [\theta_E^h | \theta_E^h \in H^{1h}(\Omega_E), \qquad \theta_E^h = g \quad \text{on } \Gamma_g] \ldots\ldots\ldots\ldots\ldots\ldots \quad (52)$$

where H^{1h} = the finite dimensional Sobolev function space, Γ_g = the Dirichlet-type boundary for Ω_E (i.e., the boundaries at $z = H + h$ and $r = h$); and g is specified according to Eqs. 18 and 19. The discrete variational formulation associated with Eq. 35 is given as follows: Find $\theta_E^h \in S^h(\Omega_E)$, such that for all $w^h \in V^h(\Omega_E)$

$$\int_{\Omega_E} w^h \frac{\partial \theta_E^h}{\partial t^*} r^* dr^* L dz^* + \int_{\Omega_E} \left(\frac{\partial w^h}{\partial r^*} \frac{\partial \theta_E^h}{\partial r^*} + \frac{1}{L^2} \frac{\partial w^h}{\partial z^*} \frac{\partial \theta_E^h}{\partial z^*} \right) r^* dr^* L dz^* = 0 \ldots\ldots \quad (53)$$

To approximate the heat flux between the reactor and the earth, we consider the layer of elements in the earth that is adjacent to the up tube of the reactor. As shown in Fig. 3, these elements involve the temperature in the up tube and the earth. The heat flux at the interface of the earth and the up tube is approximated as follows (see Fig. 3):

$$2\pi\gamma^* \left(r^* \frac{\partial \theta_E}{\partial r^*} \right) \Bigg|_{r^* = r_0^*} \doteq 2\pi\gamma^* \left(r_0^* + \frac{\Delta r^*}{2} \right) \left(\frac{\theta^+ - \theta}{\Delta r^*} \right) \ldots\ldots\ldots\ldots\ldots \quad (54)$$

Let $\Omega_F^d = (x^* | 0 \le x^* \le 1)$, $\Omega_F^s = (x^* | 0 \le x^* \le 1)$, and $\Omega_F^u = (x^* | 1 \le x^* \le 2)$ denote the one-dimensional computational domain for the reactor tubes. Further, let $\mathbf{E}_F^a$ denote the set of elements resulting from the finite element discretization of Ω_F^a into subdomains $(\Omega_F^a)^e$, $e = 1, 2, \ldots, \text{nel}_F^a$, where nel_F^a = the number of elements in the reactor tubes. The superscript a takes the value s for steam tube, d for down tube, and u for up tube. Note that at the well/earth interface $\mathbf{E}_F^u$ and $\mathbf{E}_E$ share common nodal points. We define the following finite dimensional spaces associated to $\mathbf{E}_F^a$:

$$V^{dh}(\Omega_F^d) = [w^{dh} | w^{dh} \in H^{1h}(\Omega_F^d), \qquad w^{dh} = 0 \text{ at } x^* = 0] \ldots\ldots \quad (55a)$$

$$V^{sh}(\Omega_F^s) = [w^{sh} | w^{sh} \in H^{1h}(\Omega_F^s), \qquad w^{sh} = 0 \text{ at } x^* = 0] \ldots\ldots \quad (55b)$$

$$V^{uh}(\Omega_F^u) = [w^{uh} | w^{uh} \in H^{1h}(\Omega_F^u)] \ldots\ldots\ldots\ldots\ldots\ldots\ldots\ldots \quad (55c)$$

$$S^{dh}(\Omega_F^d) = [\theta_F^{dh} | \theta_F^{dh} \in H^{1h}(\Omega_F^d), \qquad \theta_F^{dh} = 0 \text{ at } x^* = 0] \ldots\ldots \quad (56a)$$

$$S^{sh}(\Omega_F^s) = [\theta_F^{sh} | \theta_F^{sh} \in H^{1h}(\Omega_F^s), \qquad \theta_F^{sh} = \theta_0^s(t) \text{ at } x^* = 0] \ldots\ldots \quad (56b)$$

$$S^{uh}(\Omega_F^u) = [\theta_F^{uh} | \theta_F^{uh} \in H^{1h}(\Omega_F^u)] \ldots\ldots\ldots\ldots\ldots\ldots\ldots\ldots \quad (56c)$$

An additional constraint on the solution space is

$$\theta_F^{dh} = \theta_F^{sh} = \theta_F^{uh}, \qquad \text{at } x^* = 1, \qquad \forall t \ge 0 \ldots\ldots\ldots\ldots\ldots \quad (57)$$

The discrete variational forms associated with Eqs. 36–38 are given as follows: find $\theta_F^{dh} \in S^{dh}(\Omega_F^d)$, $\theta_F^{sh} \in S^{sh}(\Omega_F^s)$, $\theta_F^{uh} \in S^{uh}(\Omega_F^u)$, and $(\theta^+)^h \in S^h(\Omega_E)$ such that

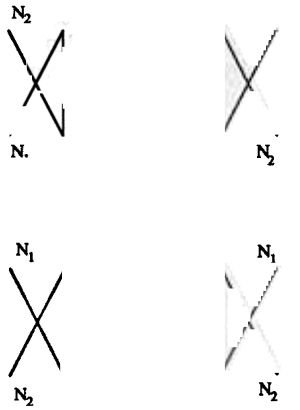

FIG. 4. Typical Pseudo-Elements: (*a*) For Up and Down Tubes; (*b*) For Down and Steam Tubes

$$\int_{\Omega_e^d} (w^{dh} + \delta^{dh}) \left[(f_p)^d \frac{\partial \theta_F^{dh}}{\partial t^*} \quad \frac{(\mathrm{Pe})^d}{L} \frac{\partial \theta_F^{dh}}{\partial x^*} + (\beta^*)^{ud} (\theta_F^{dh} - \theta_F^{uh}) d\Omega \right.$$

$$\left. + (\beta^*)^{sd} (\theta_F^{dh} \quad \theta_F^{sh}) \right] d\Omega = \int_{\Omega_F^d} (w^{dh} + \delta^{dh}) \Sigma^* d\Omega, \qquad \forall w^{dh} \in V^{dh} \tag{58}$$

$$\int_{\Omega_e^u} (w^{uh} \quad \delta^{uh}) \left[(f_p)^u \frac{\partial \theta_F^{uh}}{\partial t^*} + \frac{(\mathrm{Pe})^u}{L} \frac{\partial \theta_F^{uh}}{\partial x^*} + (\beta^*)^{ud} (\theta_F^{uh} - \theta_F^{dh}) d\Omega \right.$$

$$\left. + 2\pi\gamma^* \left(r_0^* \quad \frac{\Delta r^*}{2} \right) \left(\frac{\theta_F^{uh} - (\theta^*)^h}{\Delta r^*} \right) \right] d\Omega = 0, \qquad \forall w^{uh} \in V^{uh} \tag{59}$$

$$\int_{\Omega_F^s} (w^{s} + \delta^{sh}) \left[(f_p)^s \frac{\partial \theta_F^{uh}}{\partial t^*} + \frac{(\mathrm{Pe})^s}{L} \frac{\partial \theta_F^{uh}}{\partial x^*} + (\beta^*)^{sd} (\theta_F^{sh} - \theta_F^{dh}) \right] d\Omega$$

$$= \int_{\Omega_e^s} (w^{sh} \quad \delta^{sh}) (P^*)^s d\Omega, \qquad \forall w^{sh} \quad V^{sh} \tag{60}$$

The Petrov-Galerkin supplement function δ^h is defined as

$$\delta^h = C_{2\tau} \frac{\Delta x^*}{2} \operatorname{sign} \left(\frac{\mathrm{Pe}}{f_p} \right) \frac{\partial w^h}{\partial x^*} = c \frac{\partial w^h}{\partial \xi} \quad \ldots\ldots\ldots\ldots\ldots\ldots\ldots\ldots\ldots\ldots \tag{61}$$

where ξ = the local coordinate; $c = C_{2\tau}$ sign (Pe/f_p); and $C_{2\tau}$ = the algorithmic Courant number. Various choices for $C_{2\tau}$ can be found in Tezduyar and Ganjoo (1986). In this paper, we take $C_{2\tau} = 1$.

For the purpose of implementation, we build pseudo-elements for the reactor tubes. Each pseudo-element consists of two one-dimensional elements facing each other as shown in Fig. 4. The one-dimensional finite element shape functions are denoted by N_1 and N_2. At this point, the symbol $\mathbf{E}_F$ will also be used to denote the set of pseudo-elements. Let $\mathbf{c}_F^e$ = the (pseudo) element level heat capacity matrix; $\mathbf{k}_F^{e'}$ and $\mathbf{k}_F^{e''}$ = the (pseudo) element level matrices corresponding to the convection and the heat exchange terms, re-

spectively. These 4 × 4 matrices are given as follows. [The superscripts refer to the pseudo-elements in the steam and down tubes. The matrices f the pseudo-elements formed by the up and down tubes are given in Liou al. (1990)]:

$$(\mathbf{c}_F^e)^{sd} = \frac{\Delta x^s}{2} \begin{bmatrix} (f_p)_1^s\left(\frac{1}{2}-\frac{c}{3}\right)+(f_p)_4^s\left(\frac{1}{6}-\frac{c}{6}\right) & 0 & 0 & (f_p)_1^s\left(\frac{1}{6}-\frac{c}{6}\right)+(f_p)_4^s\left(\frac{1}{6}-\frac{c}{3}\right) \\ 0 & & & \\ 0 & & & \\ (f_p)_1^s\left(\frac{1}{6}+\frac{c}{3}\right)+(f_p)_4^s\left(\frac{1}{6}+\frac{c}{6}\right) & 0 & 0 & (f_p)_1^s\left(\frac{1}{6}+\frac{c}{6}\right)+(f_p)_4^s\left(\frac{1}{2}+\frac{c}{3}\right) \end{bmatrix} \quad (62)$$

$$(\mathbf{k}_F^e)^{sd} = \begin{bmatrix} (\mathrm{Pe})_1^s\left(-\frac{1}{3}+\frac{c}{4}\right)+(\mathrm{Pe})_4^s\left(-\frac{1}{6}+\frac{c}{4}\right) & 0 & 0 & (\mathrm{Pe})_1^s\left(\frac{1}{3}-\frac{c}{4}\right)+(\mathrm{Pe})_4^s\left(\frac{1}{6}-\frac{c}{4}\right) \\ 0 & & & \\ 0 & & & \\ (\mathrm{Pe})_1^s\left(-\frac{1}{6}-\frac{c}{4}\right)+(\mathrm{Pe})_4^s\left(-\frac{1}{3}-\frac{c}{4}\right) & 0 & 0 & (\mathrm{Pe})_1^s\left(\frac{1}{6}+\frac{c}{4}\right)+(\mathrm{Pe})_4^s\left(\frac{1}{3}+\frac{c}{4}\right) \end{bmatrix} \quad (63)$$

$$(\mathbf{k}_F^e)^{sd} = \frac{\Delta x^s}{2}(\beta^*) \begin{bmatrix} \left(\frac{2}{3}-\frac{c}{2}\right) & -\left(\frac{2}{3}-\frac{c}{2}\right) & -\left(\frac{1}{3}-\frac{c}{2}\right) & \left(\frac{1}{3}-\frac{c}{2}\right) \\ -\left(\frac{2}{3}+\frac{c}{2}\right) & \left(\frac{2}{3}+\frac{c}{2}\right) & \left(\frac{1}{3}+\frac{c}{2}\right) & -\left(\frac{1}{3}+\frac{c}{2}\right) \\ -\left(\frac{1}{3}-\frac{c}{2}\right) & \left(\frac{1}{3}-\frac{c}{2}\right) & \left(\frac{2}{3}-\frac{c}{2}\right) & -\left(\frac{2}{3}-\frac{c}{2}\right) \\ \left(\frac{1}{3}+\frac{c}{2}\right) & -\left(\frac{1}{3}+\frac{c}{2}\right) & -\left(\frac{2}{3}+\frac{c}{2}\right) & \left(\frac{2}{3}+\frac{c}{2}\right) \end{bmatrix} \quad (64)$$

where the numeric subscripts refer to the element node numbers shown in Fig. 4. The (pseudo) element level force vector due to the heat source in the down and up tubes is

$$(\mathbf{f}_F^e)^{ud} = \frac{\Delta x^s}{2} \begin{bmatrix} \left(\frac{2}{3}-\frac{c}{2}\right)\Sigma_1^* + \left(\frac{1}{3}-\frac{c}{2}\right)\Sigma_4^* \\ \left(\frac{2}{3}+\frac{c}{2}\right)\Sigma_2^* + \left(\frac{1}{3}+\frac{c}{2}\right)\Sigma_3^* \\ \left(\frac{1}{3}-\frac{c}{2}\right)\Sigma_2^* + \left(\frac{2}{3}-\frac{c}{2}\right)\Sigma_3^* \\ \left(\frac{1}{3}+\frac{c}{2}\right)\Sigma_1^* + \left(\frac{2}{3}+\frac{c}{2}\right)\Sigma_4^* \end{bmatrix} \quad (65)$$

The (pseudo) element level force vector for the steam tube is

$$(\mathbf{f}_F^e)^{sd} = \frac{}{2} \begin{bmatrix} \left(\frac{2}{3}-\frac{c}{2}\right)(P^*)_1^s + \left(\frac{1}{3}-\frac{c}{2}\right)(P^*)_4^s \\ \left(\frac{1}{3}+\frac{c}{2}\right)(P^*)_1^s + \left(\frac{2}{3}+\frac{c}{2}\right)(P^*)_4^s \end{bmatrix} \quad (66)$$

The thermodynamic quantities appearing in the element level matrices and force vector corresponding to the steam tube are calculated as described in the following

Case 1 (Saturated Steam)

Let $(p_F^s)_{A-1,n}$ and $(\rho_F^s)_{A,n-1}$ be given, where the subscripts A and n = the node and time step numbers, respectively.

1. From the pressure equation find

$$(p_F^s)_{A,n} = (p_F^s)_{A-1,n} + (\rho_F^s)_{A-1,n} g \Delta x \quad \ldots\ldots (67)$$

2. Since the fluid is in the saturation state, temperature is calculated as a function of the pressure

$$(T_F^s)_{A,n} = T_F^s[(p_F^s)_{A,n}] \quad \ldots\ldots (68)$$

Let $(\epsilon_F^s)_{A,n}^{(i)}$ be the quality of steam at the node A, at time step n, and at the end of iteration i.

3. Let

$$(\epsilon_F^s)_{A,n}^{(0)} = (\epsilon_F^s)_{A-1,n} \quad \ldots\ldots (69)$$

4. Find ρ_F^s, $(\partial \hat{h}_F^s / \partial T_F^s)_{\epsilon_F^s}$, $(\partial \hat{h}_F^s / \partial \epsilon_F^s)_{T_F^s}$ using Eqs. 12*a*–14*b*, 16*a* and 16*b* based on $(\epsilon_F^s)_{A,n}^{(i-1)}$.

5. The continuity Eq. 5 is used to calculate the mass flow rate $(\dot{m}_F^s)_{A,n}^{(i)}$.

6. Predict $(T_F^d)_{A,n}$ using the solution from the previous time step.

7. Find the modified value of quality as $(\epsilon_F^s)_{A,n}^{(i)}$ using Eq. 15.

8. Once the new value of the quality is known, go back to step 4 and iterate till some predecided convergence criterion is met. If ϵ_F^s turns out to be negative, it means that the fluid is no more in the saturation state and should be treated as a single phase fluid (case 2).

9. The temperature T_F^s and the converged value of the quality $(\epsilon_F^s)_{A,n}$ are then used to find the various coefficients in the steam-tube equation.

Case 2 (Hot Water Only)

In this case the thermodynamic properties are functions of the temperature and the pressure in the steam tube.

Let $(p_F^s)_{A-1,n}$ and $(\rho_F^s)_{A,n-1}$ be given:

1. Find $(p_F^s)_{A,n}$ using Eq. 67.
2. Predict $(T_F^s)_{A,n}$ using the solution from the previous time step.
3. Find $(\rho_F^s)_{A,n}$ using Eq. 8*b* and then $(\dot{m}_F^s)_{A,n}$ using the continuity Eq. 5.
4. Use these calculated values for temperature and pressure to calculate the desired coefficients in the steam tube equation.

With the aid of the definition of the pseudo-elements in the reactor tubes and the associated element level matrices, the assembly procedure for the global matrices is straightforward. Let $\mathbf{E}_A$ denote the subset of elements in $\mathbf{E}_E$ that are adjacent to the well/earth interface. The assembly procedure is performed as

$$\mathbf{C} = \mathop{\mathbf{A}}_{e \in \mathbf{E}_E} \mathbf{c}_E^e + \mathop{\mathbf{A}}_{e \in \mathbf{E}_F} [(\mathbf{c}_F^e)^{ud} + (\mathbf{c}_F^e)^{sd}] \quad \ldots\ldots (70)$$

$$\mathbf{K} = \mathop{\mathbf{A}}_{e \in \mathbf{E}_E} \mathbf{k}_E^e + \mathop{\mathbf{A}}_{e \in \mathbf{E}_F} [(\mathbf{k}_F^{e'})^{ud} + (\mathbf{k}_F^{e''})^{ud} + (\mathbf{k}_F^{e'})^{sd} + (\mathbf{k}_F^{e''})^{sd}] + \mathop{\mathbf{A}}_{e \in \mathbf{E}_A} \mathbf{k}_F^{e'''} \quad \ldots\ldots (71)$$

$$\mathbf{F} = \mathop{\mathbf{A}}_{e \in \mathbf{E}_E} \mathbf{f}_E^e + \mathop{\mathbf{A}}_{e \in \mathbf{E}_F} [(\mathbf{f}_F^e)^{ud} + (\mathbf{f}_F^e)^{sd}] \quad \ldots\ldots (72)$$

where $\mathbf{A}$ = the assembly operator that permutes the element level matrices and adds them to the global matrices. The element level heat capacity and conductivity matrices corresponding to Eq. 53 are represented by $\mathbf{c}_E^e$ and $\mathbf{k}_E^e$, whereas the element level force vector is represented by $\mathbf{f}_E^e$. $\mathbf{k}_F^{e''}$ = the element level contribution due to the heat flux at the well/earth interface and must be added to the conductivity matrix for those elements in the earth that are adjacent to the reactor (Liou et al. 1990). The assembly of the element level arrays leads to a set of ordinary differential equations and initial conditions

$$\mathbf{Cv} + \mathbf{Kd} = \mathbf{F} \quad \ldots\ldots (73)$$

$$\mathbf{d}(0) = \mathbf{d}_0 \quad \ldots\ldots (74)$$

where $\mathbf{C}$ and $\mathbf{K}$ = the global capacity and conductivity matrices; and $\mathbf{F}$ = the force vector. The vectors $\mathbf{d}$ and $\mathbf{v}$ = the unknown nodal values of the temperature and its time derivative. The ordinary differential Eq. 73 with its initial condition Eq. 74 is solved by a predictor/multicorrector algorithm (Liou et al. 1990).

Numerical Examples

The method described was tested on the simulation of the start-up in a model deep-well reactor for three different cases. A mesh with 2,128 nodal points and 1,925 two-dimensional and 150 one-dimensional (100 pseudo-elements) elements was used. The physical values for the processes for all cases are

$$r_0 = 0.1585 \text{ m} \quad \ldots\ldots (75)$$

$$H = 1{,}524 \text{ m} \quad \ldots\ldots (76)$$

$$h = 3.048 \text{ m} \quad \ldots\ldots (77)$$

$$T_E^0(z) = 26.667^\circ \text{C} + 0.0292 \frac{z}{\text{m}} {}^\circ\text{C} \ .$$

$$(\rho C_p)_E = 2.681 \frac{\text{MJ}}{\text{m}^3 \cdot {}^\circ\text{C}}$$

$$\kappa = 1.7296 \frac{\text{J}}{\text{m} \cdot \text{s} \cdot {}^\circ\text{C}}$$

$$(A\rho C_p)_P^a = 16.88 \frac{\text{kJ}}{\text{m} \cdot {}^\circ\text{C}}$$

$$(A\rho C_p)_P^u = 55.42 \frac{\text{kJ}}{\text{m} \cdot {}^\circ\text{C}}$$

$$(A\rho C_p)_P^s = 2.285 \frac{\text{kJ}}{\text{m} \cdot {}^\circ\text{C}}$$

$$(A\rho C_p)_F^d = 100.76 \frac{\text{kJ}}{\text{m} \cdot {}^\circ\text{C}}$$

$$(A\rho C_p)_F^u = 126.24 \frac{\text{kJ}}{\text{m} \cdot {}^\circ\text{C}}$$

$$(\dot{m}C_p)_F^d = 76{,}776.71 \frac{\text{J}}{\text{s} \cdot {}^\circ\text{C}} \quad \ldots\ldots (86)$$

$$\sigma^{sd} = 0.649 \frac{\text{m}^2}{\text{m}} \quad \ldots (87)$$

$$\sigma^{id} = 0.916 \frac{\text{m}^2}{\text{m}} \quad (88)$$

$$U^{sd} = 851.17 \frac{\text{J}}{\text{s} \cdot \text{m}^2 \cdot {}^\circ\text{C}} \quad \ldots (89)$$

$$U^{id} = 56.74 \frac{\text{J}}{\text{s} \cdot \text{m}^2 \cdot {}^\circ\text{C}} \quad \ldots\ldots (90)$$

We are interested in the temperature profile in the tubes and the heat loss to the earth as a function of time. The temperature attained at the bottom of the reactor and the exit temperature are the two significant quantities. The former will control the maximum conversion achieved and the phase behavior of solids in the system during the actual operation. The latter is a measure of the heat removed by the exit stream, which will control the amount of useful heat recoverable.

Case 1

We start up the reactor by introducing steam (at temperature $T_0^s = 315.6°$ C and quality $\epsilon_0^s = 0.95$) at the inlet of the steam tube at a mass flow rate of $\dot{m}_F^s = 2.52$ kg/s. In the steam tube, steam condenses as it flows down the tube, but it has a nonzero quality when it reaches the bottom of the reactor. There it condenses upon mixing with the down-tube fluid and releases the heat of vaporization. In this example, we assume that the heat released by the condensation of the vapor is evenly distributed over the last element length (30.48 m) in the down tube. We can relax this assumption later when we have a better understanding of the mixing of the two fluid streams at the bottom of the reactor. In this case the fluid temperature in the steam tube increases as it goes down the tube. This is because in the saturation state the temperature is a function of the pressure, which increases due to the hydrostatic gradient down the tube. Fig. 5 shows the temperature profiles in the tubes during the start-up and the temperature contours in the earth at the end of 12 hours. No oscillations in the temperature in the tubes are observed. This illustrates that the convection-dominance of the equation in the tubes does not pose any numerical difficulty in our approach. At the end of 12 hours, the bottom temperature in the well reaches 314.4° C, which is adequate to obtain high oxidation rate and good overall conversion. The exit temperature is 61.1° C (Fig. 6).

Case 2

This time we start up the reactor by introducing steam again, but of lower quality (at temperature $T_0^s = 315.6°$ C and quality $\epsilon_0^s = 0.55$), at the inlet of the steam tube at a mass flow rate of $\dot{m}_F^s = 2.52$ kg/s. In this case, steam condenses completely as it flows down the steam tube before it reaches the bottom of the reactor. The fluid temperature down the steam tube first increases while it is in the saturation state and then decreases after it has con-

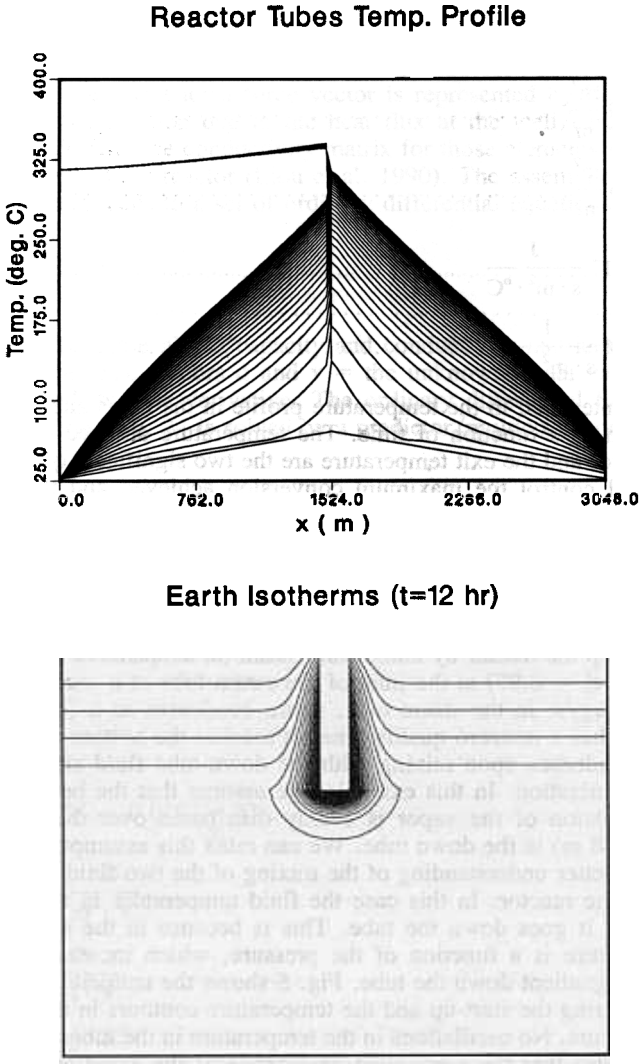

FIG. 5. Temperature Profiles in Reactor Tubes During 0–12 hr and Isotherms in Earth at End of Start-Up Using High-Quality Steam (315.6° C, Quality: 0.95) Injected at 2.52 kg/s (Case 1)

densed completely. Fig. 7 shows the temperature profiles in the tubes during the start-up and the temperature contours in the earth at the end of 12 hours. At the end of the start-up, the bottom temperature in the well reaches 236.1° C, which is much less than that in case 1. The exit temperature is 55° C (Fig. 8).

Case 3

We start up the reactor by introducing hot water (at temperature T_0 =

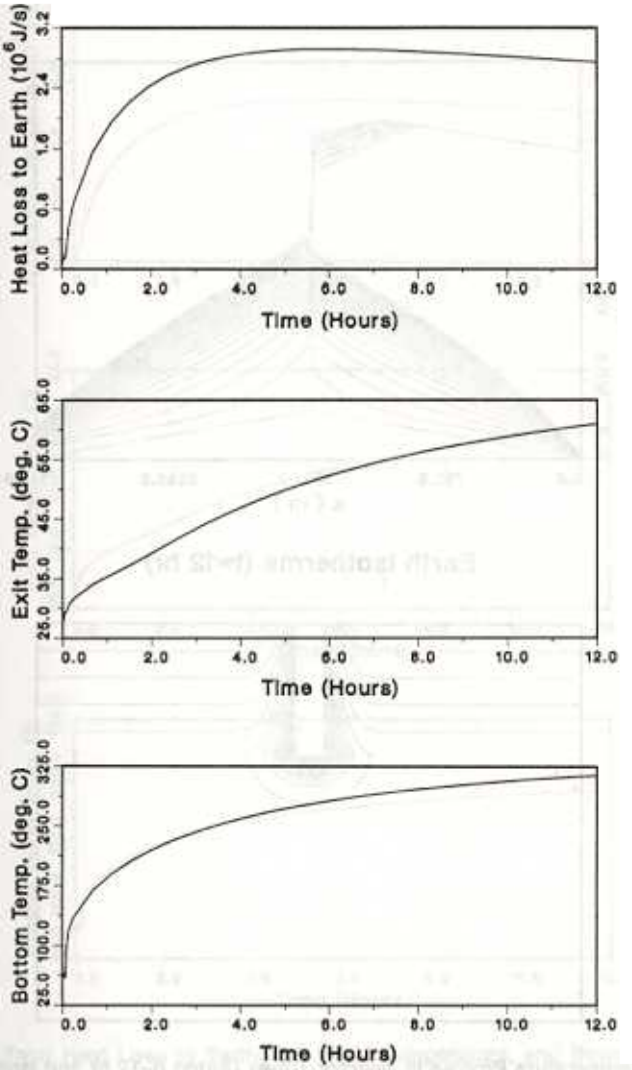

FIG. 6. Total Heat Loss to Earth, Exit Fluid Temperature, and Bottom Temperature of Reactor versus Time During Start-Up Using High-Quality Steam (315.6° C, Quality: 0.95) Injected at 2.52 kg/s (Case 1)

260° C and pressure p_0^s = 4.826 MPa) at the inlet of the steam tube at a mass flow rate of $\dot{m}_F^s$ = 4.977 kg/s. This time the fluid temperature down the steam tube decreases all the way to the bottom. Fig. 9 shows the temperature profiles in the tubes during the start-up and the temperature contours in the earth at the end of 12 hours, for this case. At the end of the start-up, the bottom temperature in the well reaches 195.6° C, which, as expected, is much less than that in cases 1 and 2. This temperature is probably not

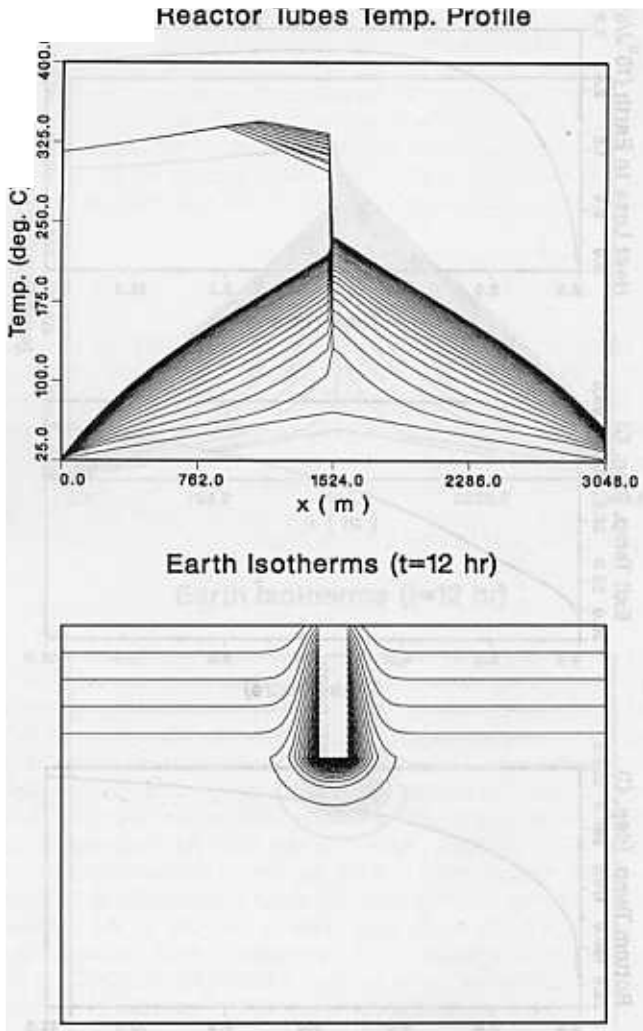

FIG. 7. Temperature Profiles in Reactor Tubes During 0–12 hr and Isotherms in Earth at End of Start-Up Using Low-Quality Steam (315.6° C, Quality: 0.55) Injected at 2.52 kg/s (Case 2)

high enough to obtain a good overall conversion. The exit temperature is 58.9° C (Fig. 10).

Conclusions

A finite element model is developed for the numerical simulation of the start-up of a deep-well wet oxidation reactor. The model can simulate start-up using saturated steam of arbitrary quality, including hot water (i.e., quality = 0). Thermodynamic relations are included for the start-up fluid in the steam tube to evaluate the necessary material properties. A Petrov-Galerkin

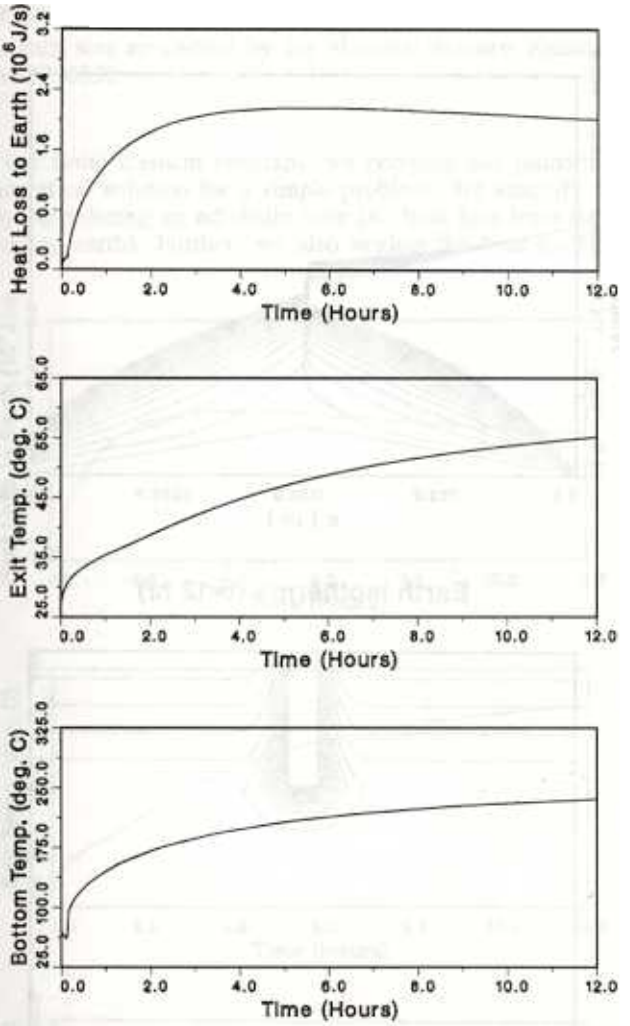

FIG. 8. Total Heat Loss to Earth, Exit Fluid Temperature, and Bottom Temperature of Reactor versus Time During Start-Up Using Low-Quality Steam (315.6° C, Quality: 0.55) Injected at 2.52 kg/s (Case 2)

method is used for the spatial discretization of the governing equations for the temperature in the reactor tubes and a regular Galerkin method for the conductive heat equation in the earth. The two equation sets are coupled by the continuity of the temperature and heat flux at the interface between the earth and the well. A predictor-multicorrector algorithm is used for the temporal discretization.

Numerical tests were performed for the start-up of a model reactor using high-pressure saturated steam and high-temperature water. The injection of high-pressure steam of sufficiently high quality seems to be good enough to obtain high oxidation rate and good overall conversion. This study can also

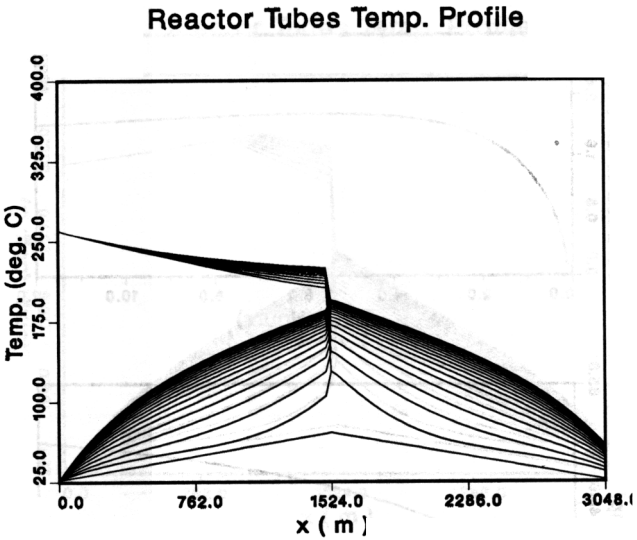

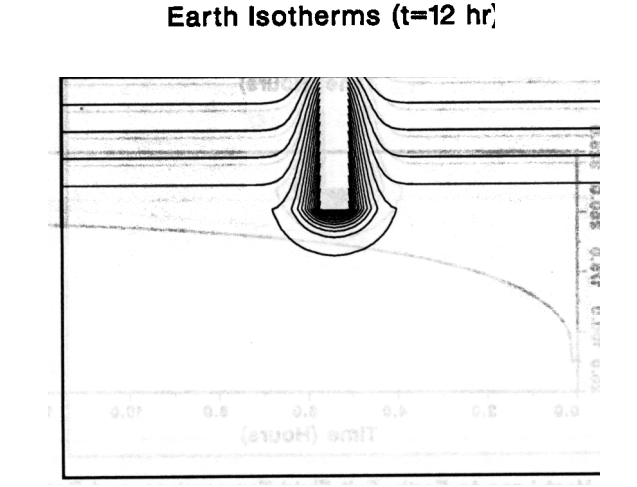

FIG. 9. Temperature Profiles in Reactor Tubes During t=12 hr and Isotherms in Earth at End of Start-Up Using Hot Water (260° C, Pressure: 4.826 MPa) Injected at 4.977 kg/s (Case 3)

be used to estimate the start-up time and the mass of the steam or water required in the start-up process.

Further improvements are possible in the present model. Pressure equations for the down and up tubes can be included so that the assumption of constant material properties in those tubes can be relaxed. Real kinetics of the mixing of the aqueous streams at the bottom of the reactor can also be introduced. The transition from start-up to steady operation of the reactor can also be studied.

Acknowledgments

This research was sponsored by the National Science Foundation under grant MSM-8796352.

Appendix I.

To test our finite element program, we compare our numerical solution with the analytical solution for a simple problem. We simplify the original problem by considering an adiabatic case (no heat loss from the reactor to the surrounding earth). Further, we also neglect the heat transfer between

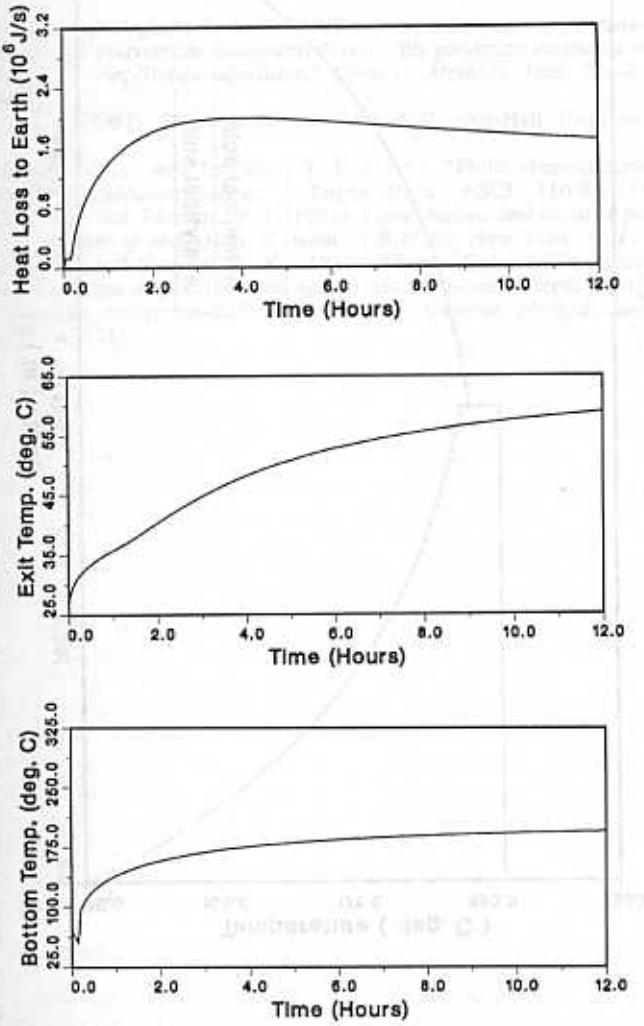

FIG. 10. Total Heat Loss to Earth, Exit Fluid Temperature, and Bottom Temperature of Reactor versus Time During Start-Up Using Hot Water (260° C, Pressure: 4.826 MPa) Injected at 4.977 kg/s (Case 3)

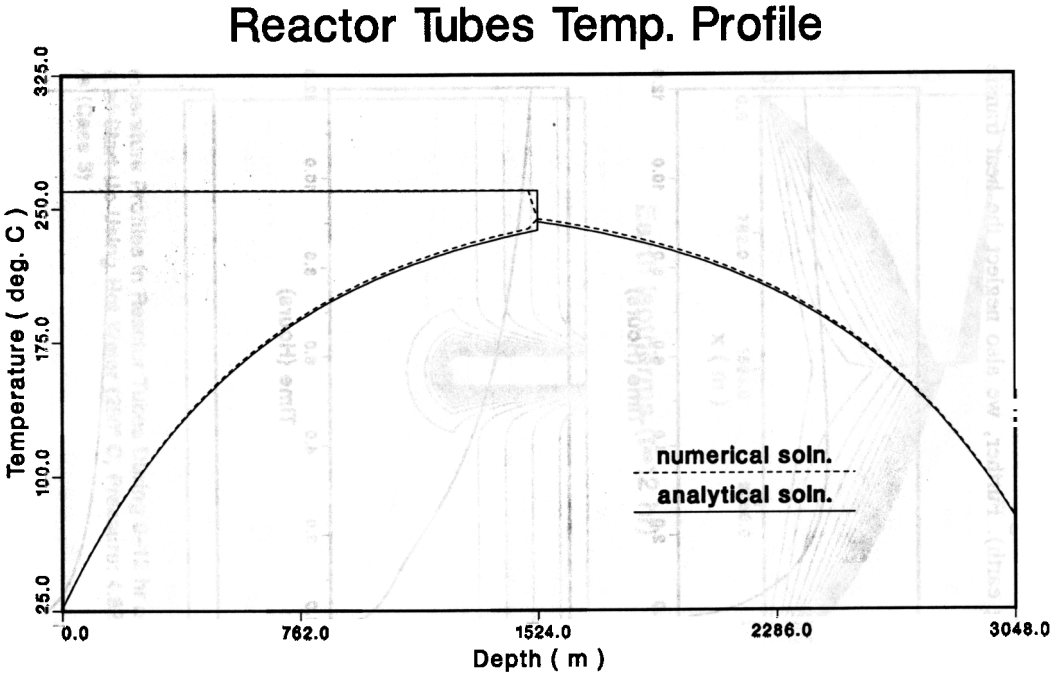

FIG. 1 Steady State Numerical and Analytical Solutions for Simplified Adiabatic Problem; Start-Up Using Hot Water (260° C, Pressure: 4.826 MPa) Injected at 4.977 kg/s

the steam and down tubes and focus on the steady-state limit for the start-up using hot water (assumed incompressible to get the analytical solution).

For this test we inject hot water (at temperature $T_0^s = 260°$ C and pressure $p_0^s = 4.826$ MPa) at the inlet of the steam tube at a mass flow rate of $\dot{m}_F^s = 4.977$ kg/s (as in Case 3). The analytical solution and our numerical solution, to this test problem, have been plotted in Fig. 11. As can be seen, the two solutions are very close. This confirms the validity of our formulation and the reliability of our program.

Appendix II. References

Brooks, A. N., and Hughes, T. J. R. (1982). "Streamline upward/Petrov-Galerkin formulations for convection dominated flows with particular emphasis on the incompressible Navier-Stokes equations." *Comput. Methods Appl. Mech. Engrg.*, 32, 199–259.

Hughes, T. J. R. (1987). *The finite element method.* Prentice-Hall, Englewood Cliffs, N. J.

Liou, J., Deans, H. A., and Tezduyar, T. E. (1990). "Finite element simulation of a deep-well wet oxidation reactor." *J. Engrg. Mech.*, ASCE, 116(8), 1780–1797.

McLintock, R. B., and Silvestri, G. J. (1968). *Formulations and iterative procedures for the calculation of properties of steam.* A.S.M.E., New York, N.Y.

Tezduyar, T. E., and Ganjoo, D. K. (1986). "Petrov-Galerkin formulations with weighting functions dependent upon spatial and temporal discretization: Application to transient convection-diffusion problems." *Comput. Methods Appl. Mech. Engrg.*, 59, 47–71.